

# Specific heat of an $S=1/2$ Heisenberg ladder compound

## $\text{Cu}_2(\text{C}_5\text{H}_{12}\text{N}_2)_2\text{Cl}_4$ under magnetic fields

M. Hagiwara and H. A. Katori

*RIKEN (The Institute of Physical and Chemical Research), Wako, Saitama 351-0198, Japan*

U. Schollwöck

*Sektion Physik, Ludwig-Maximilians-Universität München, Theresienstr. 37, 80333 München,  
Germany*

H. -J. Mikeska

*Institut für Theoretische Physik, Universität Hannover, Appelstr. 2, D-30167 Hannover,  
Germany*

(Received )

### Abstract

Specific heat measurements down to 0.5 K have been performed on a single crystal sample of a spin-ladder like compound  $\text{Cu}_2(\text{C}_5\text{H}_{12}\text{N}_2)_2\text{Cl}_4$  under magnetic fields up to 12 T. The temperature dependence of the observed data in a magnetic field below 6 T is well reproduced by numerical results calculated for the  $S=1/2$  two-leg ladder with  $J_{\text{rung}}/J_{\text{leg}}=5$ . In the gapless region above 7 T ( $H_{c1}$ ), the agreement between experiment and calculation is good above about 2 K and a sharp and a round peak were observed below 2 K in a magnetic field around 10 T, but the numerical data show only a round peak, the magnitude of which is smaller than that of the observed one. The origin of the sharp peak and the difference between the experimental and numerical

round peak are discussed.

75.40-s,75.40.Cx,75.40.Mg,75.10.Jm

## I. INTRODUCTION

Recently, there has been a considerable interest in quantum spin systems with a spin gap above the singlet ground state. One of the examples studied extensively are one dimensional Heisenberg antiferromagnets (1DHAFs) with integer spin values, especially spin( $S$ ) one, which is associated with Haldane's prediction [1]. Now, these studies extend those of the  $S=1$  antiferromagnetic bond alternating chains [2,3]. Another case is  $S=1/2$  two leg spin-ladder which is investigated as an intermediate system between one- and two-dimensional systems [4,5]. Spin-ladder systems have been studied in relation to the Haldane problem on one hand [6,7] and high  $T_c$  superconductivity on the other hand [8,9]. Most of the spin-ladder systems investigated so far are copper oxides [5,10]. One of remarkable things is that a lightly hole doped two leg ladder exhibits superconductivity under high pressure [9,11] as expected theoretically [4]. On the other hand, spin-ladder like copper complexes  $\text{Cu}_2(\text{C}_5\text{H}_{12}\text{N}_2)_2\text{Cl}_2$  (abbreviated as CHpC) [12–19] and  $\text{KCuCl}_3$  and its family compounds [20–22] have been also studied extensively. These compounds except for  $\text{NH}_4\text{CuCl}_3$  [21] have the singlet ground state and become gapless at a certain magnetic field ( $H_{c1}$ ). The features of this gapless region at low temperatures have attracted much interest because the field induced long range ordering (LRO) in  $\text{TlCuCl}_3$  [22] has been interpreted as a Bose-Einstein condensation of magnons [23]. This matter was originally argued by Affleck [24] that the ground state above  $H_{c1}$  may be regarded as a Bose condensate of the low energy boson. Besides, the dimensionality is expected to appear in the power-law dependences of thermodynamic quantities on temperature, when approaching the quantum critical point by application of a magnetic field [25]. Furthermore, in the quantum critical region above the LRO temperature, we can investigate the feature of Tomonaga-Luttinger(TL) liquid for a quasi one-dimensional antiferromagnet [26,27].

The compound CHpC has been studied extensively for several years by various experiments such as magnetic susceptibility [12–14], magnetization [12–14], NMR [15,16], ESR [14,17], specific heat [12,18,19] and neutron scattering measurements [12]. From these ex-

periments, CHpC has the singlet ground state with an excitation gap of about 10 K and the gap collapses at about 7 T ( $H_{c1}$ ) and the saturation field is about 13 T ( $H_{c2}$ ). This compound has an advantage of study on the gapless spin liquid phase under magnetic fields, because  $H_{c1}$  and  $H_{c2}$  are easily accessible fields with a conventional superconducting magnet. Specific heat measurements in a magnetic field were done up to 9 T by Hammer *et al.* [12] and up to 8.25 T by Calemczuk *et al.* [18]. In the present paper, we extend the specific heat measurements under magnetic fields up to 12 T beyond the symmetry field  $H_{\text{sym}}(=(H_{c1}+H_{c2})/2)$  and compare the experimental results with those of numerical and analytical calculations.

The format used in this paper is as follows: In Sec. II, experimental and theoretical details are described. Experimental results of magnetic susceptibility and specific heat under magnetic fields( $H$ ) are reported in comparison with some numerical calculations in Sec. III. A sharp and a round peak observed at low temperatures in the gapless region are discussed in Sec. IV.

## II. EXPERIMENTAL AND NUMERICAL DETAILS

Powder samples of CHpC were synthesized according to the method reported in Ref.[26]. Equimolar amounts of 1,4-diazacycloheptane ( $C_5H_{12}N_2$ ) and  $CuCl_2 \cdot 2H_2O$  were dissolved in warm methanol (60°C) for 1 hour and left at room temperature for two days. Single crystals of CHpC were obtained by the slow evaporation method from a methanol solution of powder samples of CHpC. We obtained samples with  $2 \times 2 \times 1$  mm<sup>3</sup> in typical size.

CHpC crystallizes in the monoclinic system and belongs to the  $P2_1/c$  space group [28]. The lattice constants and  $\beta$  angle at room temperature are  $a=13.406(3)\text{\AA}$ ,  $b=11.454(2)\text{\AA}$ ,  $c=12.605(3)\text{\AA}$  and  $\beta=115.01(2)^\circ$ . Cu dimeric units are linked to the neighboring ones via hydrogen bonds along the [101] direction. The upper panel of Fig. 1 shows a schematic view of the chain like structure along [101] of CHpC. Broken lines in the upper panel show the hydrogen bonds and the ellipsoids around the copper atoms represent the 3d hole orbitals.

In the lower panel of Fig. 1, possible pathways of the exchange interaction between the neighboring  $\text{Cu}^{2+}$  spins are depicted. The exchange interaction on the broken pathway must be much weaker than those on the other pathways because of the configuration of 3d copper and 3p chlorine orbitals, thus considering this system as the  $S=1/2$  two leg spin-ladder.

Magnetic susceptibilities ( $M/H$ ) were measured with a SQUID magnetometer (Quantum Design's MPMS2) in RIKEN. Specific heat measurements down to 0.5 K under magnetic fields up to 12 T were performed with Mag Lab<sup>HC</sup> micro calorimeter (Oxford Instruments) installed at the same place. The relaxation method was employed so that we used only one single crystal with 4.3 mg in weight. Numerical calculations were done by the temperature-dependent density-matrix-renormalization-group (DMRG) method for the  $S=1/2$  two-leg Heisenberg spin-ladder with a spin Hamiltonian written as

$$\mathcal{H} = J_{rung} \sum_{j=1}^{N/2} \mathbf{S}_{1,j} \cdot \mathbf{S}_{2,j} + J_{leg} \sum_{i=1}^2 \sum_{j=1}^{N/2} \mathbf{S}_{i,j} \cdot \mathbf{S}_{i,j+1} - g\mu_B H \sum_{i,j} S_{i,j}^z, \quad (1)$$

where  $J_{rung}$  and  $J_{leg}$  are the exchange constants along the rung and the leg, respectively and  $\mathbf{S}_{i,j}$  an  $S=1/2$  spin on the  $i$ -th leg, the  $j$ -th rung,  $g$  the  $g$ -value of copper,  $\mu_B$  the Bohr magneton and  $H$  the external magnetic field. As we use a transfer matrix approach, it is free of finite size effects.

### III. EXPERIMENTAL RESULTS AND COMPARISON WITH CALCULATIONS

#### A. Magnetic susceptibility

Solid circles of Fig. 2 shows the temperature dependence of magnetic susceptibility of a single crystal sample of CHpC along the chain direction. A hump which is typical of low dimensional antiferromagnets is observed around 10 K and the susceptibility steeply decreases with further decrease of temperature toward zero Kelvin. No increase of the susceptibility due to magnetic impurity or crystal defect is observed in this sample. The solid line in this figure is a fit of the calculated susceptibilities to the experimental ones with the fitting parameters of  $g=2.1$ ,  $J_{rung}=13.1$  K and  $J_{leg}=2.62$  K ( $J_{rung}/J_{leg}=5$ ). The agreement

between numerical and experimental susceptibilities is excellent. Evaluated values and the ratio of the exchange constants are close to those estimated by other groups [12,13]. In the following comparison of specific heat, we use the same fitting parameters.

### B. Specific heat at $H=0$ T

In Fig. 3, filled circles represent raw specific heat data. Usually the lattice part of the specific heat is evaluated from the specific heat of a nonmagnetic isomorphous compound. But no isomorphous compound with nonmagnetic atom like Zn exists. In order to get the magnetic contribution of the specific heat, we subtract the lattice part ( $C_{\text{lattice}}$ ) of the specific heat from the raw data in the standard way, assuming  $C_{\text{lattice}} \sim T^3$  at low temperatures. The broken line in Fig. 3 is the lattice part of the specific heat with a coefficient of 0.004 (J/K Cu-mol) which is not far from those evaluated in other copper complexes (*e.g.* 0.0048 for  $(\text{CH}_3)_2\text{CHNH}_3\text{CuCl}_3$  [29]). Open circles show the subtracted results, namely, magnetic part of the specific heat and we see a round peak due to the short range ordering around 5 K. The solid line represents the specific heat at  $H=0$  T calculated with the same fitting parameters as the susceptibility fitting. The calculated specific heat satisfactorily agrees with the observed one. At the temperature below the round peak, an exponential decay due to a spin gap is observed. We fit the specific heat data at low temperatures to an expression of  $C_{\text{mag}} \sim T^{-3/2} \exp(-\Delta/T)$  to evaluate the energy gap. This expression is deduced in the low temperature limit for the strong coupling case ( $J_{\text{rung}}/J_{\text{leg}}=5$ ) approximating the dispersion  $J_{\text{rung}} + J_{\text{leg}} \cos \tilde{q}$  where  $\tilde{q}$  is the component of wave vector transfer along the chain [12]. The fitting result is drawn as the solid line in Fig.4 with the fitting parameter  $\Delta=10.9$  K, which is very close to the value of  $J_{\text{rung}} - J_{\text{leg}} (=10.48$  K).

### C. Specific heat at $H \neq 0$ T

Filled symbols in Figs. 5(a), 5(b) and 5(c) show the magnetic specific heat data for magnetic fields below  $H_{c1}$ , between  $H_{c1}$  and  $H_{\text{sym}}$  and above  $H_{\text{sym}}$ , respectively. In Figs.5(a),

5(b) and 5(c), a hump is observed above 5 K at each designated magnetic field. Moreover, we observed two peaks below 2 K near  $H_{\text{sym}}$  in Figs.5(b) and 5(c). Details of this low temperature part are depicted in the upper panel of Fig.6. We obviously see two peaks, a sharp and a round peak at the magnetic field above 8.5 T. In this figure, we plot the specific heat data under 10.5T for simplicity. Figure 7 shows the magnetic field dependence of the specific heat. Two peaks are observed below 0.82 K (only one peak at 0.61 K because of our instrumental limitation), whereas no peak is observed at 0.87 K. We plot these two peaks at low temperatures in Figs.5-7 in the plane of  $H$  vs.  $T$  of Fig. 8. Plotted points are almost symmetric at  $H_{\text{sym}}(\sim 10$  T) for both peaks.

Next, we compare the experimental data with the numerical ones. Solid, broken, dotted lines in each figure of Fig.5 represent the numerical specific heat data for the designated magnetic fields. In Fig.5(a), the agreement between experimental and numerical specific heat is excellent over the entire temperature range up to 9 K. In Figs.5(b) and 5(c), the agreement between experiment and calculation is good above 2 K, while the large deviation is seen below about 2 K. In the lower panel of Fig. 6, calculated specific heat data are displayed for the magnetic fields corresponding to those in the upper panel. The tendency of the calculated round peak to shift with change of fields is similar to the observed one, but the magnitude of the peak is much smaller than that of the observed peak. We show in Fig.9 the magnitude of the round peak as a function of magnetic field. The field at the calculated maximum peak slightly shifts to the lower side compared to the experimental one. The magnitude of the calculated peak is almost a half of the observed one.

Entropy of this sample is calculated from the specific heat data shown in the upper panel of Fig.10 for the designated magnetic field. Correspondingly, we show the calculated entropy for the corresponding magnetic field in the lower panel of Fig.10. Similar tendency of the entropy is observed in both figures. With increasing the magnetic fields, the entropy becomes higher at low temperatures. This behavior is opposite to that in a paramagnet.

#### IV. DISCUSSION AND CONCLUSIONS

First let us discuss the origin of the sharp peak observed in the experiment. Usually, the sharp peak is thought to be caused by magnetic long range ordering (LRO) [27], but it is controversial for the case of a spin ladder; for example, it predicts a field dependence of the transition temperature (camel-type structure) contrary to experimental observations (dromendary-type structure). Recently, Nagaosa and Murakami [30] argued that a lattice instability in the spin ladder is expected to occur above  $H_{c1}$ . From their study, the lattice distortion occurs in the spin ladder at an incommensurate wave vector corresponding to the magnetization.

For a comparison of these scenarios with our experiment, we note that the one of the experimental consequences of Nagaosa's and Murakami's scenario is that a gap should appear below the transition temperature ( $T_c$ ) and the specific heat should behave as  $C \sim \exp(-\gamma v_0/T)$ , where  $\gamma v_0$  is the gap of the order of  $T_c$ . In the upper panel of Fig.11, we fit the experimental data at 10 T below the temperature at the sharp peak to this equation and obtained fairly good agreement between them with  $\gamma v_0=2.58$  K, which is however quite far from the temperature  $T_c$  of about 0.8 K at 10 T. If the sharp peak is on the other hand caused by antiferromagnetic long range order, the magnetic part of the specific heat should go as  $T^3$  due to the antiferromagnetic magnons. We show the fitting result using this equation in the lower part of Fig.11. The agreement between experiment and calculation is comparably good to the previous fitting, when we add a constant. This negative contribution is however unexplained. Both interpretations are therefore not really conclusive, and discrepancies remain between the possible sources of the sharp peak and the specific heat data, calling for the proposal of a new transition scenario.

Theoretically we can discuss the round peak based on a fermion representation. The round peak can be attributed to the low energy excitation structure in a gapless spin liquid (TL liquid). As pointed out in the related context of mixed spin 1 and  $\frac{1}{2}$  by Kolezhuk *et.al.* [31], the round peak arises from a spinon band in the spin liquid system. They reduce the



Hilbert space of the problem, keeping only the most important states per elementary cell. In the strong coupling case of the spin ladder, this amounts to keeping for each rung only the singlet and the lowest-energy triplet component around  $H_{c1}$ , mapping them to an effective spin 1/2 chain [26,27]. Then the effective Hamiltonian is given by

$$\mathcal{H} = J_{leg} \sum_{i=1}^N (s_i^x \cdot s_{i+1}^x + s_i^y \cdot s_{i+1}^y + 1/2 s_i^z \cdot s_{i+1}^z) - (g\mu_B H - J_{rung} - 1/2 J_{leg}) \sum_{i=1}^N s_i^z, \quad (2)$$

where  $s_i^x$ ,  $s_i^y$  and  $s_i^z$  are the  $x$ ,  $y$  and  $z$  component of the effective 1/2 spin. When, for a qualitative consideration, the  $s_i^z \cdot s_{i+1}^z$  term is neglected, the remaining free fermion hamiltonian can be easily treated. Then a splitting of the peak is expected to occur [31] due to contributions from two different spinon bands (particle and hole band) for magnetic fields off the symmetry field  $H_{sym}$ . In experiment and in numerical studies on the full original Hamiltonian of the ladder, we however observe only one peak, which is probably due to the large deviation of the effective Hamiltonian from the exactly solvable xy-limit, making the analytical prediction of a peak split less stringent.

Finally, the difference of the magnitude between the experimental and the numerical round peak has to be discussed. When calculating the specific heat, we neglected the diagonal exchange interaction denoted by  $j$  in Fig. 1. This interaction can possibly affect the nature of the specific heat at low temperatures, but it should not allow for an effect of more than 50 percent as observed. There must be an additional source of entropy and disorder, probably related to the physics driving the three dimensional transition, which at present can only be speculated about.

In conclusion, we have made specific heat measurements on a single crystal sample of the  $S=1/2$  Heisenberg spin-ladder compound  $\text{Cu}_2(\text{C}_5\text{H}_{12}\text{N}_2)_2\text{Cl}_2$  under magnetic fields. Experimental data are compared to the numerical ones calculated with a temperature dependent DMRG method for the  $S=1/2$  spin-ladder and are well reproduced when  $H < H_{c1}$ , but when  $H > H_{c1}$  and for temperatures below about 2 K the magnitude of the observed round peak differs by a factor of about 2. The numerical calculations give quasiexact results for the 1D Hamiltonian considered in the whole temperature and magnetic field range. The remaining

discrepancies have therefore to be due to effects beyond that Hamiltonian, probably due to low-temperature 3D coupling and/or further degrees of freedom (such as phonons), as also indicated by the 3D transition.

We have observed two peaks, a sharp and a round peak at low temperatures below 2 K around  $H_{\text{sym}}$ . The origin of the former peak is still controversial and two possibilities are discussed: the antiferromagnetic LRO [27] and the lattice instability above  $H_{\text{c1}}$  proposed by Nagaosa and Murakami [30]. The latter peak probably comes from a spinon band in the effective Tomonaga-Luttinger liquid. A simple analytical fermion representation predicts moreover a weak splitting of the round peak into two round peaks for magnetic fields off the symmetry field  $H_{\text{sym}}$ , but experimental and numerical results show consistently only one peak. This shows that on the analytical level a more elaborate analysis of the Hamiltonian is needed to describe the round peak in the 1D picture, while qualitatively the emergence of a new low-temperature structure in the specific heat is well captured.

#### ACKNOWLEDGMENTS

We would like to thank K. Katsumata for access to the SQUID magnetometer and Mag Lab<sup>HC</sup> calorimeter system. M. H. expresses his thanks to J. -P. Boucher, N. Nagaosa and K. Totsuka for fruitful discussions. This work was partially supported by a Grant-in-Aid for Science Research from the Japanese Ministry of Education, Science, Sports and Culture. Thanks are also due to the Chemical Analysis and the Molecular Characterization Units in RIKEN.

## REFERENCES

- [1] F. D. M. Haldane, Phys. Lett. **93** A, 464 (1983); Phys. Rev. Lett. **50**, 1153 (1983).
- [2] M. Hagiwara, Y. Narumi, K. Kindo, M. Kohno, H. Nakano, R. Sato and M. Takahashi, Phys. Rev. Lett **80**, 1312 (1998).
- [3] Y. Narumi, M. Hagiwara, R. Sato, K. Kindo, H. Nakano and M. Takahashi, Physica B **246-247**, 509 (1998).
- [4] T. M. Rice, S. Gopalan, M. Sigrist, Europhys. Lett. **23**, 445 (1993).
- [5] M. Azuma, Z. Hiroi, M. Takano, K. Ishida, Y. Kitaoka, Phys. Rev. Lett. **73**,3463 (1994).
- [6] K. Hida, J. Phys. Soc. Jpn. **60**, 1347 (1991).
- [7] H. Watanabe, K. Nomura and S. Takada, J. Phys. Soc. Jpn. **62**, 2845 (1993).
- [8] E. Dagotto and T. M. Rice, Science **271**, 618 (1996).
- [9] M. Uehara, T. Nagata, J. Akimitsu, H. Takahashi, N. Mōri and K. Kinoshita, J. Phys. Soc. Jpn. **65**, 2764 (1996).
- [10] M. Matsuda and K. Katsumata, Phys. Rev. B**53**, 12261 (1996).
- [11] T. Nagata, M. Uehara, J. Goto, J. Akimitsu, N. Motoyama, N. Mōri, Phys. Rev. Lett. **81**, 1090 (1998).
- [12] P. R. Hammer, D. H. Reich and C. Broholm, Phys. Rev. B**57**, 7846 (1998).
- [13] G. Chaboussant, P. A. Crowell, L. P. Lévy, O. Piovesana, A. Madouri and D. Mailly, Phys. Rev. B**55**, 3046 (1997).
- [14] M. Hagiwara, Y. Narumi, K. Kindo, T. Nishida, M. Kaburagi and T. Tonegawa, Physica B**246-247**, 234 (1998).
- [15] G. Chaboussant, M.-H. Julien, Y. Fagot-Revurat, M. Hanson, L. P. Lévy, C. Berthier, M. Horvatić and O. Piovesana, Eur. Phys. J. B**6**, 167 (1998).

- [16] M. Chiba, T. Fukui, Y. Ajiro, M. Hagiwara, T. Goto and T. Kubo, *Physica B* **246-247**, 576 (1998).
- [17] H. Ohta, T. Tanaka, S. Okubo, S. Kimura, H. Kikuchi and H. Nagaosa, *J. Phys. Soc. Jpn.* **68**, 732 (1999).
- [18] R. Calemczuk, J. Riera, D. Poilblanc, J.-P. Boucher, G. Chaboussant, L. P. Lévy and O. Piovesana, *Eur. Phys. J. B* **7**, 171 (1999).
- [19] M. Hagiwara, H. A. Katori, U. Schollwöck, H.-J. Mikeska, in Proc. of the 22nd conference on Low Temperature Physics, Helsinki, 1999 (to appear in *Physica B*).
- [20] H. Tanaka, K. Takatsu, W. Shiramura and T. Ono, *J. Phys. Soc. Jpn.* **65**, 1945 (1996).
- [21] K. Takatsu, W. Shiramura and H. Tanaka, *J. Phys. Soc. Jpn.* **66**, 1611 (1997).
- [22] A. Oosawa, M. Ishii and H. Tanaka, *J. Phys.: Condens. Matter.* **11**, 265 (1999).
- [23] T. Nikuni, M. Oshikawa, A. Oosawa and H. Tanaka, preprint, cond-mat/9908118.
- [24] I. Affleck, *Phys. Rev. B* **41**, 6697 (1990).
- [25] N. Elstner and R. R. P. Singh, *Phys. Rev. B* **58**, 11484 (1998).
- [26] F. Mila, *Eur. Phys. J. B* **6**, 201 (1998).
- [27] T. Giamarchi and A. Tsvelik, *Phys. Rev. B* **59**, 11398 (1998).
- [28] B. Chiari, O. Piovesana, T. Tarantelli and P. F. Zanazzi, *Inorg. Chem.* **29**, 1172 (1990).
- [29] H. Manaka, I. Yamada, Z. Honda, H. A. Katori and K. Katsumata, *J. Phys. Soc. Jpn.* **67**, 3913 (1998).
- [30] N. Nagaosa and S. Murakami, *J. Phys. Soc. Jpn.* **67**, 1876 (1998).
- [31] A. K. Kolezhuk, H.-J. Mikeska, K. Maisinger and U. Schollwöck, *Phys. Rev. B* **59**, 13565 (1999).

## FIGURES

FIG. 1. A schematic view of the chain structure of  $\text{Cu}_2(\text{C}_5\text{H}_{12}\text{N}_2)_2\text{Cl}_4$  and the exchange pathways. Broken lines represent hydrogen bonds and ellipsoids show 3d hole orbitals of copper.

FIG. 2. Temperature dependence of magnetic susceptibilities of a single crystal of  $\text{Cu}_2(\text{C}_5\text{H}_{12}\text{N}_2)_2\text{Cl}_4$  along the chain direction ( $[101]$ ). The solid line represents calculated susceptibilities for the  $S=1/2$  Heisenberg spin-ladder with the fitting parameters shown in the panel.

FIG. 3. Specific heat as a function of temperature at  $H=0$  T. Filled circles are raw specific heat data and a broken line represents the estimated lattice part of the specific heat. Open circles show the magnetic specific heat. The solid line represents the specific heat calculated for the  $S=1/2$  spin ladder with the same fitting parameters as the susceptibility.

FIG. 4. Specific heat at  $H=0$  T in the plane of  $\ln[C_{\text{mag}}T^{3/2}]$  vs.  $1/T$ . The solid line is the result of a fit to the equation  $\sim T^{3/2}\exp(-\Delta/T)$  with  $\Delta=10.9$  K.

FIG. 5. Temperature dependence of the specific heat under the designated magnetic fields along  $[101]$  direction. The solid, broken and dotted lines are calculated specific heat data for the corresponding magnetic fields.

FIG. 6. Details of the specific heat as a function of temperature at low temperatures below 1.5 K above  $H_{c1}$ .

FIG. 7. Magnetic field dependence of the specific heat along the  $[101]$  direction for the designated temperatures. Solid lines are guides for the eye.

FIG. 8. Plot of the peaks of the specific heat at low temperatures above 7 T in the magnetic field *vs.* temperature plane. Filled circles and open squares correspond to the sharp peaks and the round ones, respectively. Solid lines are guides for the eye.

FIG. 9. Magnitude of the round peak as a function of magnetic field. Filled circles and open squares represent the magnetic specific heat data for experiment and calculation, respectively. Solid lines are guides for the eye.

FIG. 10. (a) Entropy as a function of temperature calculated from the observed specific heat data for designated magnetic fields. The entropy at the lowest temperature of about 0.5 K is evaluated as half of  $C_{\text{mag}}$  at the lowest temperature. (b) Calculated entropy as a function of temperature corresponding to the experiment. Solid lines are guides for the eye.

FIG. 11. (a) Specific heat data at 10 T in the plane of  $-\ln C_{\text{mag}}$  versus  $1/T$ . The solid line represents a fit of the experimental data to an equation  $\sim \exp(-\gamma v_0/T)$ . (b) Specific heat data at 10 T in the plane of  $C_{\text{mag}}$  versus  $T^3$ . The solid line shows a fit of the experimental data to an equation  $a+bT^3$  where  $a$  and  $b$  are fitting parameters.

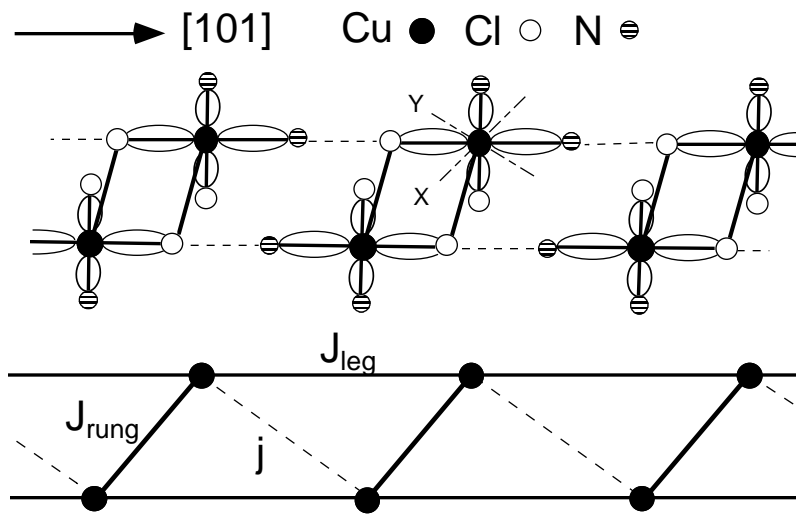


Fig.1 M. Hagiwara et al.

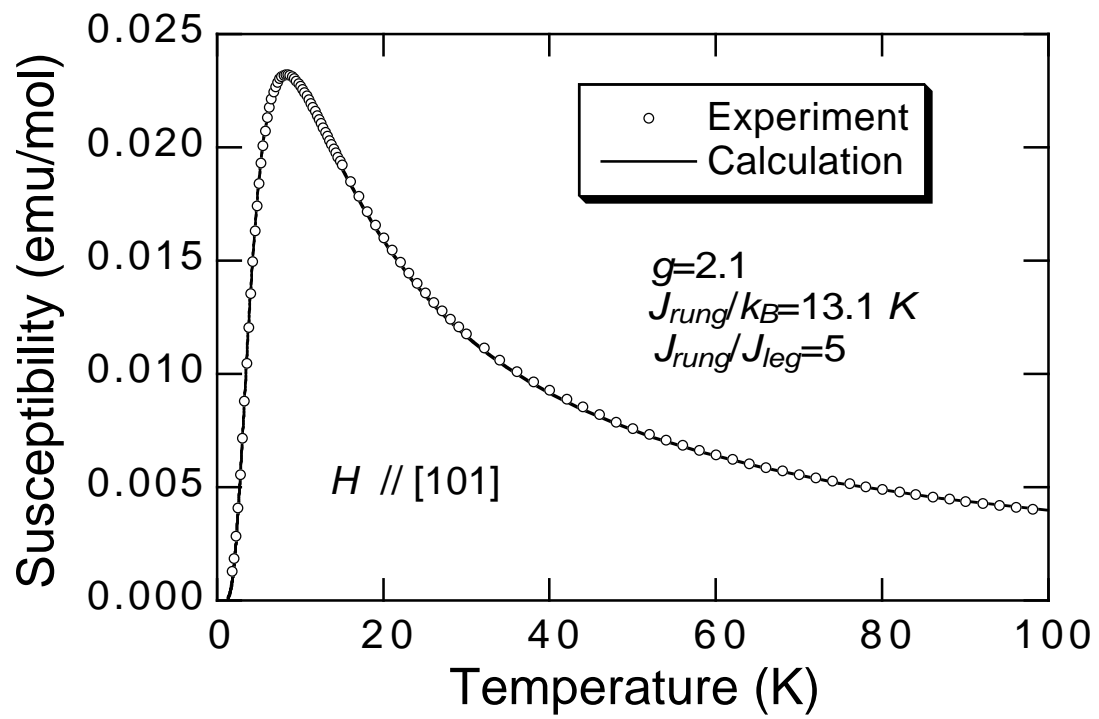


Fig.2 M. Hagiwara et al.



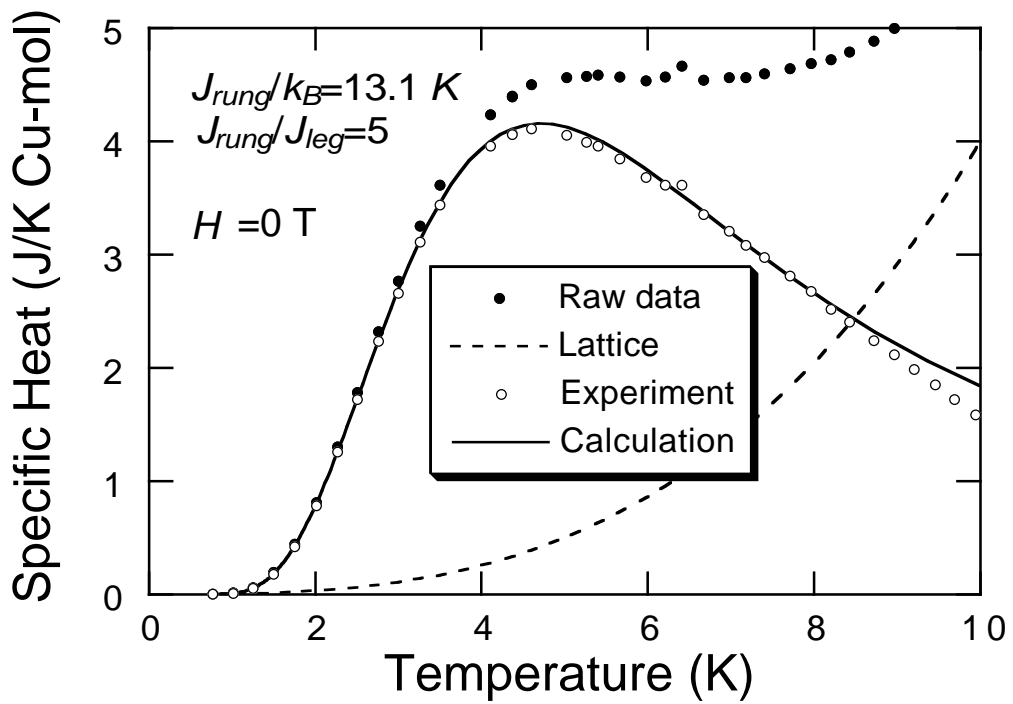


Fig. 3 M. Hagiwara et al.

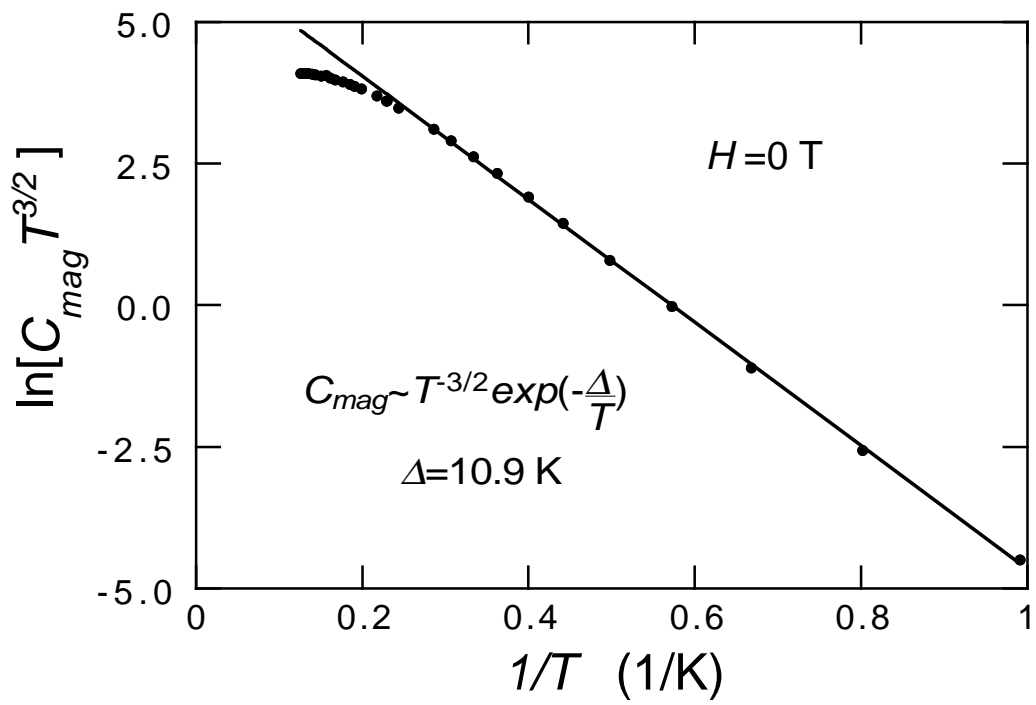


Fig. 4 M. Hagiwara et al.

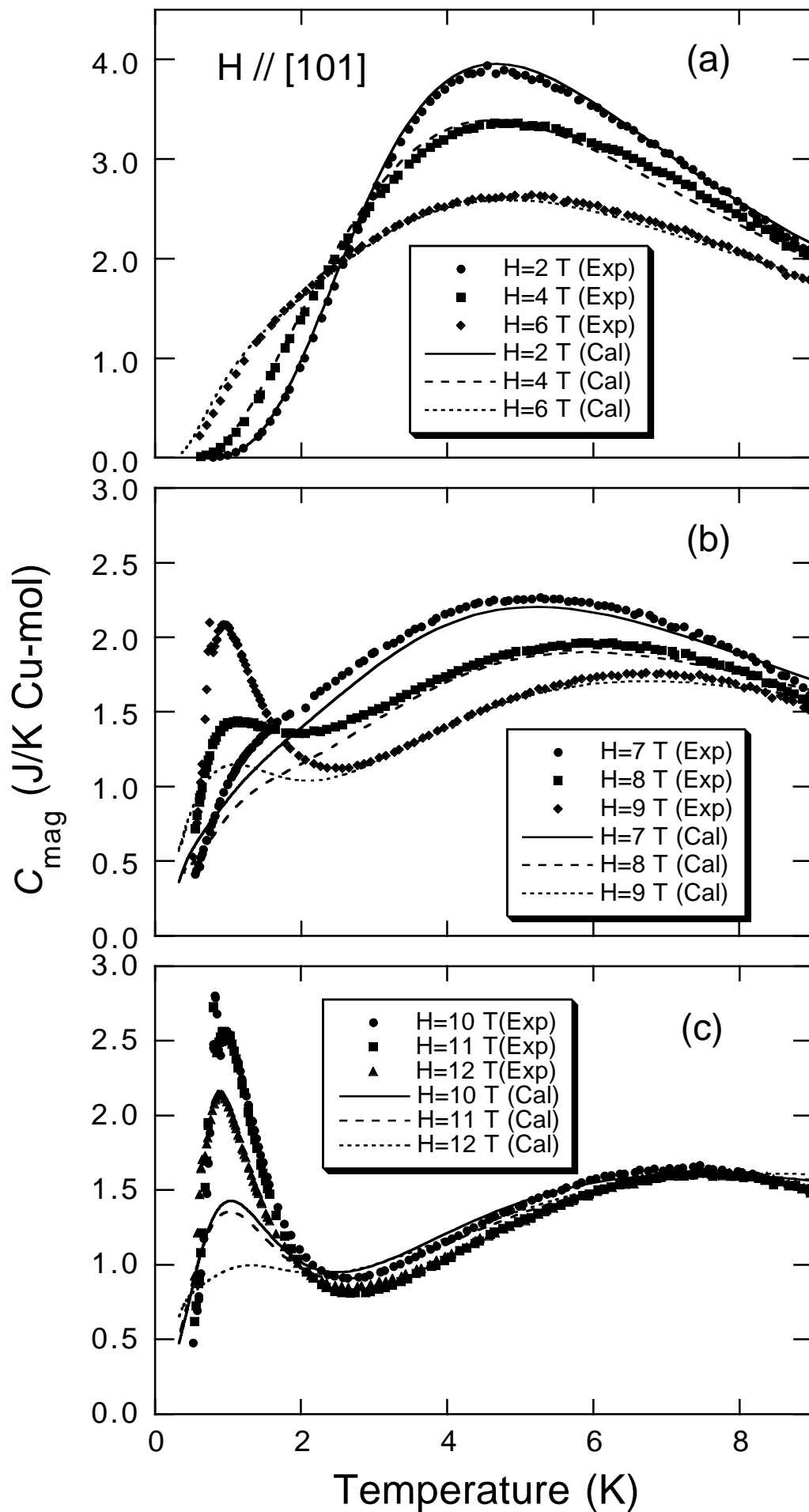


Fig. 5 M. Hagiwara et al.

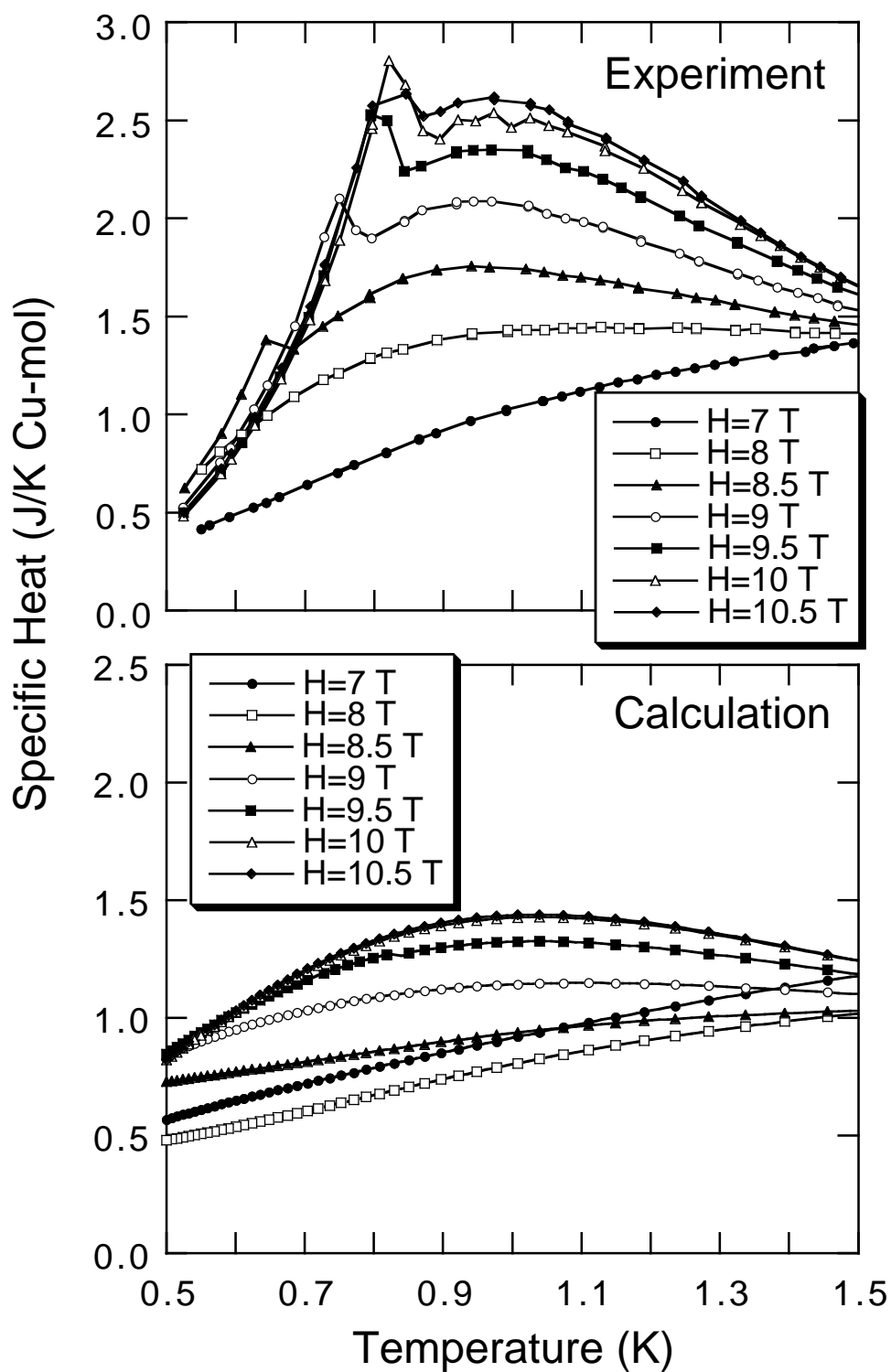


Fig.6 M. Hagiwara et al.

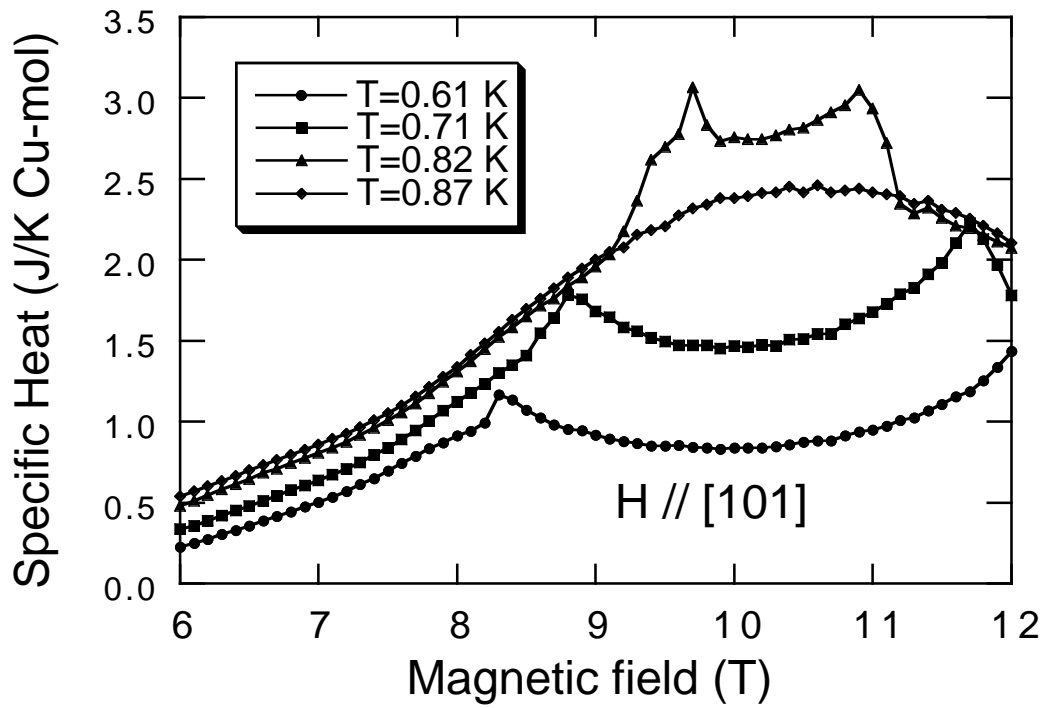


Fig. 7 M. Hagiwara et al.

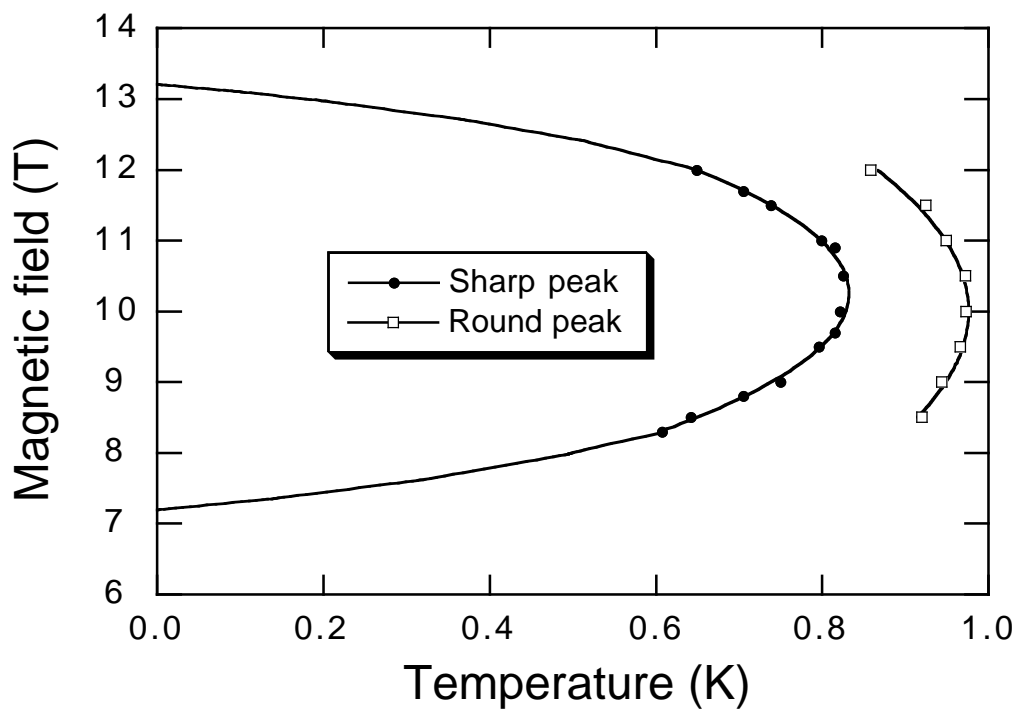


Fig.8 M. Hagiwara et al.

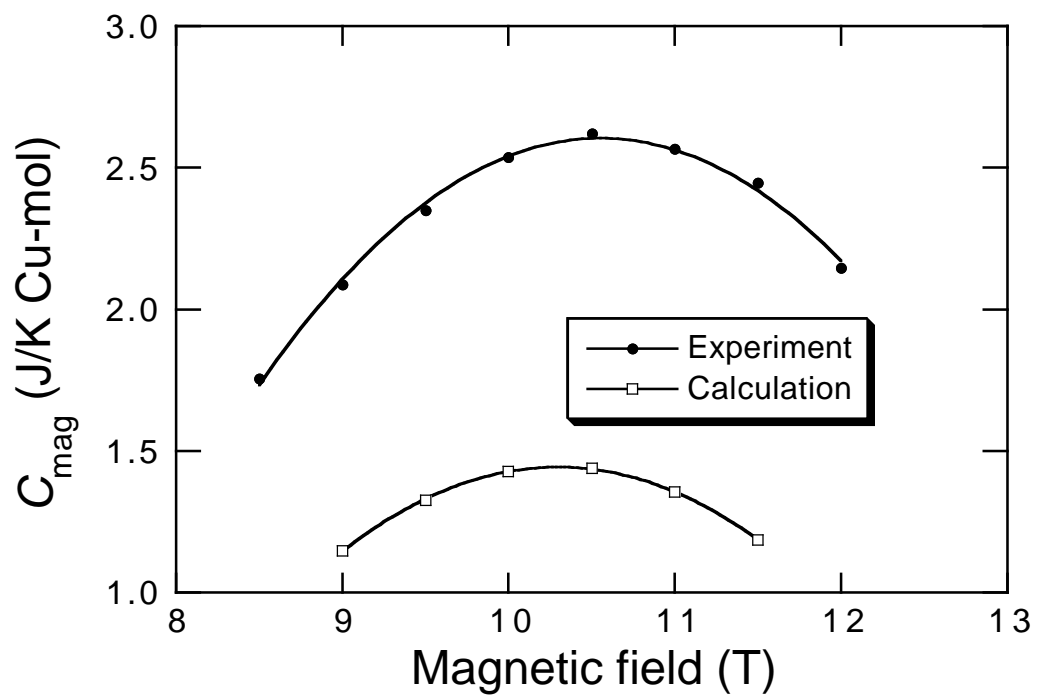


Fig. 9 M. Hagiwara et al.

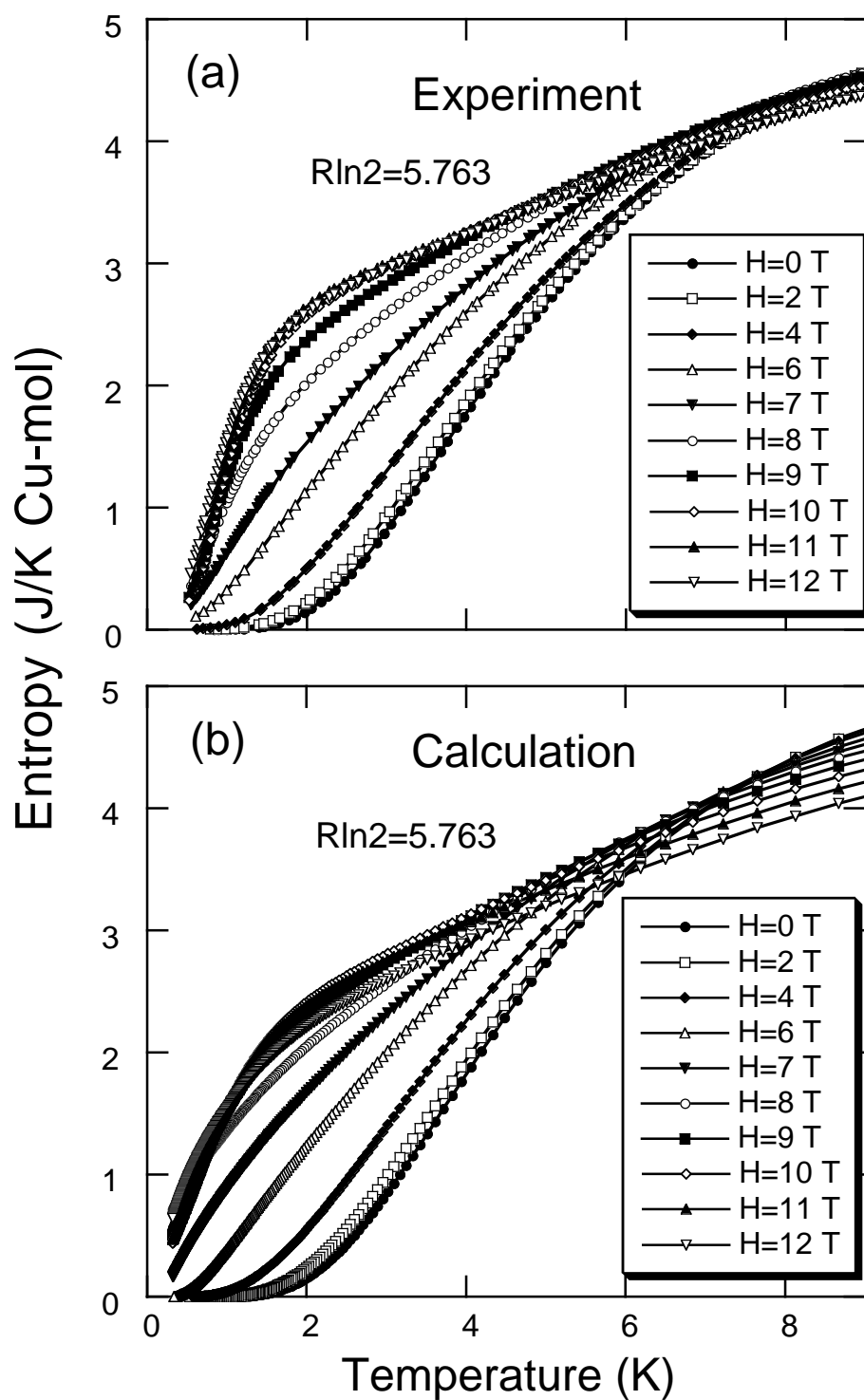


Fig. 10 M. Hagiwara et al.



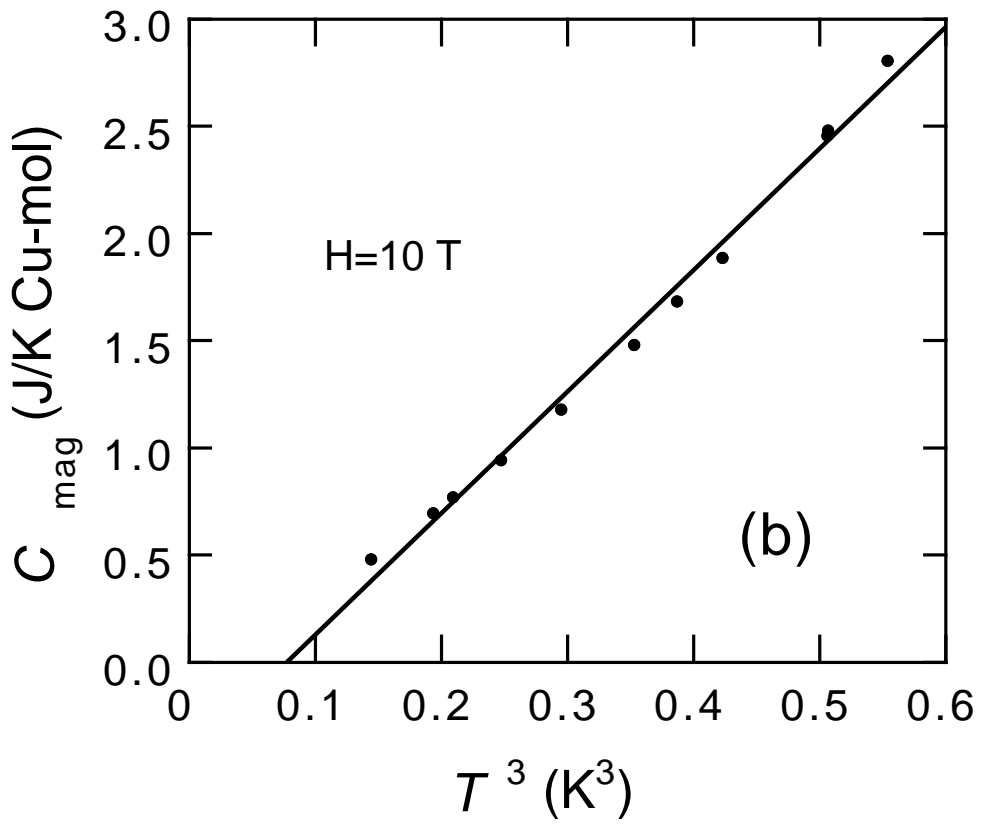
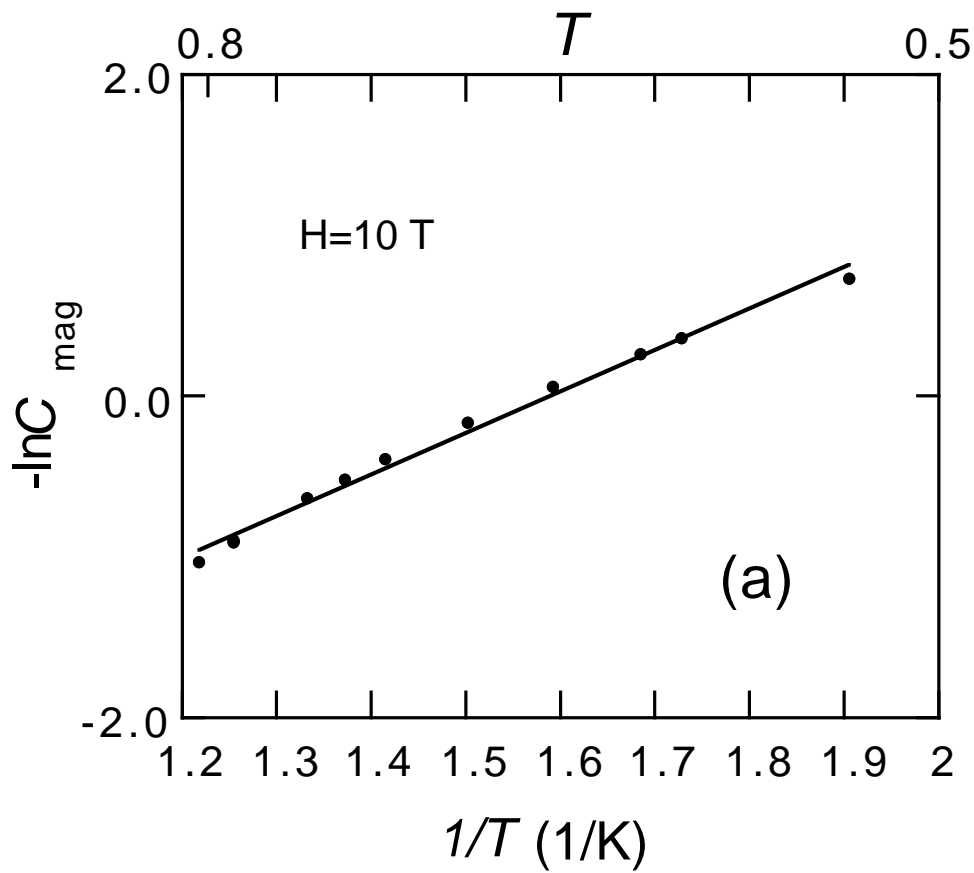


Fig. 11 M. Hagiwara et al.